

## Metallic Foams

International Edition: DOI: 10.1002/anie.201804932

German Edition: DOI: 10.1002/ange.201804932

***hcp*-Co Nanowires Grown on Metallic Foams as Catalysts for Fischer–Tropsch Synthesis**

Justine Harmel, Laurent Peres, Marta Estrader, Adrien Berliet, Sylvie Maury, Antoine Fécant, Bruno Chaudret, Philippe Serp,\* and Katerina Soulantica\*

**Abstract:** The Fischer–Tropsch synthesis (FTS) is a structure-sensitive exothermic reaction that enables catalytic transformation of syngas to high quality liquid fuels. Now, monolithic cobalt-based heterogeneous catalysts were elaborated through a wet chemistry approach that allows control over nanocrystal shape and crystallographic phase, while at the same time enables heat management. Copper and nickel foams have been employed as supports for the epitaxial growth of *hcp*-Co nanowires directly from a solution containing a coordination compound of cobalt and stabilizing ligands. The Co/Cu<sub>foam</sub> catalyst was tested for Fischer–Tropsch synthesis in a fixed-bed reactor, showing stability and significantly superior activity and selectivity towards C<sub>5</sub>+ compared to a Co/SiO<sub>2</sub>-Al<sub>2</sub>O<sub>3</sub> reference catalyst under the same conditions. ■■ Abstract was too long ■■

**B**oth fossil and renewable resources can be converted into liquid fuels using XTL (X-To-Liquid) technologies, where X can be natural or shale gas, coal, or biomass.<sup>[1]</sup> This technology is based on carbon source reforming or gasification to produce syngas, which is further transformed via the Fischer–Tropsch synthesis (FTS) and upgrading into liquid fuels suitable for transportation.<sup>[2]</sup>

The high-temperature (300–350 °C) FTS process is used for the production of gasoline and linear low-molecular-mass olefins, and uses mainly iron-based catalysts.<sup>[3]</sup> The low-temperature (200–240 °C) process is used for the production of higher-molecular-mass linear hydrocarbons, which are then hydrotreated to produce diesel and jet fuels. Nowadays, the most employed active phase for the low-temperature FTS is metallic cobalt, either pure or promoted by trace amounts of noble metals.<sup>[3,4]</sup> As far as the Co catalyst structure is concerned, a cobalt particle size effect has been evidenced. For Co particles smaller than 6 nm, a decreased TOF and

increased methane selectivity have been reported.<sup>[5]</sup> Besides the particle size, the catalytic performance has been proposed to depend significantly on the cobalt crystallographic phase.<sup>[6]</sup> Density functional theory-based kinetic studies have shown that for CO dissociation in the presence of hydrogen, which is identified as the rate limiting step of FTS, *hcp*-Co catalysts have remarkably higher intrinsic activity than the *fcc*-Co catalysts, and follow a direct dissociation route, while the *fcc*-Co catalysts prefer a H-assisted route.<sup>[7]</sup> The formation of *hcp*-cobalt was also experimentally found to be the key for an improved catalytic activity in FT catalysis,<sup>[8]</sup> however, the selective preparation of an *hcp*-Co catalyst with the requested particle size is still a challenging task.<sup>[9]</sup>

FTS being highly exothermic, it is also important to rapidly dissipate the heat of reaction from the catalyst particles in order to avoid overheating, which will lead to increased deactivation rate by sintering and fouling, as well as to the undesirable production of methane.<sup>[10]</sup> In this context, the use of metallic structured supported catalysts<sup>[11]</sup> is particularly appealing. It has been proposed that micro-reactors, with enhanced mass and heat transfers and excellent mixing, could potentially improve the productivity and reduce methane formation in FTS.<sup>[12]</sup> Up to now, only wash-coated catalysts are employed. Provided that the wash-coat thickness is sufficiently thin, these catalysts can insure: i) short diffusion distances and low pressure drop for the reaction, and ii) high thermal conductivity to enable isothermal operation. A simpler and more efficient approach could be the direct growth of the metallic active phase on a metallic support, especially if its active surface and its structure are controlled. This can be achieved by employing wet chemistry approaches for the catalyst elaboration.

Cobalt nanorods (NRs) and nanowires (NWs) crystallized in the *hcp* structure have already been produced by some of us by reduction in solution under H<sub>2</sub> of the [Co{N(SiMe<sub>3</sub>)<sub>2</sub>}-2-(thf)}]<sup>[13]</sup> precursor in the presence of long chain amine and acid stabilizers.<sup>[14]</sup> These *hcp*-cobalt NWs/NRs can also be grown on various crystallographically oriented metallic substrates by solution epitaxial growth.<sup>[15]</sup> Interestingly, these NWs could also be grown on commercial Cu foils, which are characterized by a random crystallographic orientation of their surface. These results inspired us for the synthesis of monolithic heterogeneous catalysts in which the catalytic phase is directly grown on metallic foams.

Herein, we show that *hcp*-Co NWs can be selectively grown on metallic foams, giving rise to nanostructured monoliths. Taking into account the potential superior performance of *hcp* Co, as well as the fact that the robust metal–metal interface between the support and the Co particles

[\*] Dr. J. Harmel, L. Peres, Dr. M. Estrader, Dr. B. Chaudret, Dr. K. Soulantica

LPCNO, Université de Toulouse, CNRS, INSA, UPS  
135 avenue de Rangueil, 31077 Toulouse (France)  
E-mail: ksoulant@insa-toulouse.fr

Dr. J. Harmel, Prof. Dr. P. Serp  
LCC-CNRS, Université de Toulouse, CNRS, INPT  
Toulouse (France)  
E-mail: pserp@nesiacet.fr

A. Berliet, Dr. S. Maury, Dr. A. Fécant  
IFP Energies Nouvelles  
Rond-point de l'échangeur de Solaize, 69360 Solaize (France)

Supporting information and the ORCID identification number(s) for the author(s) of this article can be found under:  
<https://doi.org/10.1002/anie.201804932>.

should allow stabilizing the particles towards sintering and optimizing heat exchanges in the reactor, we have investigated the *hcp*-Co/Cu<sub>foam</sub> monolith as a nanostructured catalyst in the FTS, achieving performances that surpass that of a Co/Al<sub>2</sub>O<sub>3</sub>-SiO<sub>2</sub> reference catalyst in terms of catalyst activity and selectivity.

Details of the material synthesis procedures are described in the Supporting Information. Briefly, the Co NWs were grown from a solution containing [Co{N(SiMe<sub>3</sub>)<sub>2</sub>}(thf)], hexadecylamine (HDA), and lauric acid (LA), which was heated under H<sub>2</sub> at 150 °C in the presence of the metallic foam. The main characteristics and scanning electron microscopy (SEM) micrographs of the copper foam before Co growth are given in Figure S1. After Co growth, dense arrays of Co NWs are visible on the foam surface (Figure 1).

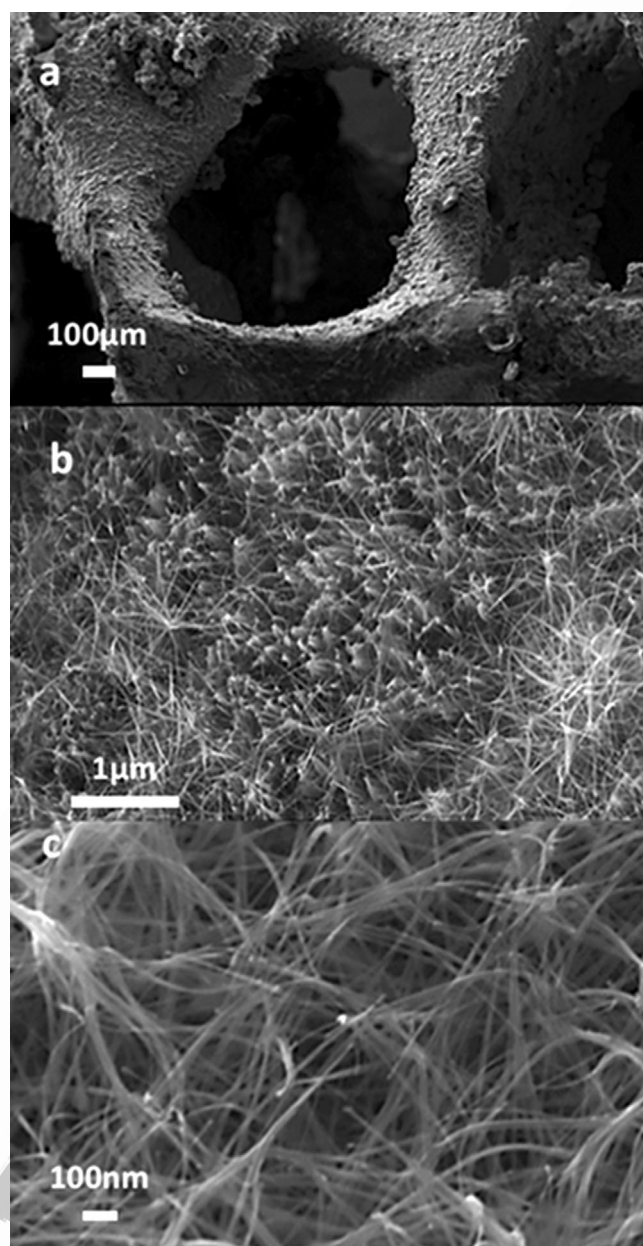


Figure 1. SEM images of the Co/Cu<sub>foam</sub>: a) general aspect; b),c) larger magnifications.

The presence of overgrown Co can also be confirmed by the change of color of the foam (Supporting Information, Figure S2a). The cobalt NWs length is estimated from SEM observations to be around 1 μm (Supporting Information, Figure S2b) and their diameter around 15 nm. ICP-AES analyses of the cobalt content in the hybrid material show a cobalt loading of 0.25% w/w. Magnetic measurements under inert conditions performed on this material evidence the purely metallic character of cobalt, since no exchange bias is observed in the field cooled hysteresis cycle (Supporting Information, Figure S3).<sup>[16]</sup> These measurements have also allowed the estimation of the residual organic ligand amount (around 8% w/w with respect to Co). As expected from the low Co content of the sample, the X-ray diffraction (XRD) pattern of the Co/Cu<sub>foam</sub> material shown in Figure 2 and

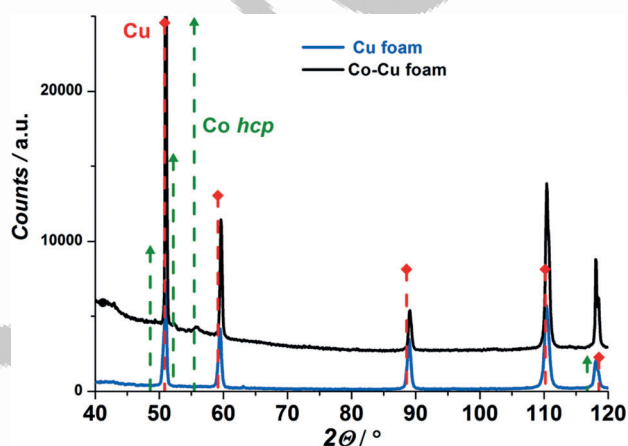


Figure 2. XRD diagrams of the Cu foam (blue line), and the Co NWs grown on the Cu foam (black line).

obtained under inert conditions displays low intensity peaks attributed to *hcp*-Co, and intense peaks for copper. X-Ray photoelectron spectroscopy (XPS) analyses have been performed on the Cu foam and the Co/Cu<sub>foam</sub> material (Supporting Information, Figures S4). We note that the CuO peaks observed on the as received copper foam disappeared after cobalt growth, which is presumably due to the reduction of the oxide layer during the Co growth under H<sub>2</sub>. The absence of CuO peaks in the XRD diffractogram of the Cu foam indicates that the CuO observed by XPS corresponds to a very thin layer. The cobalt phase is essentially Co<sup>0</sup>, and the small amounts of CoO are present due to the air-exposure during preparation of the XPS sample.

The thermal stability of the Co/Cu<sub>foam</sub> was evaluated via a heat treatment at 350 °C for 3 hours under Ar/H<sub>2</sub> flow (93:7). The SEM images obtained after the heat treatment show no change in the morphology of the cobalt NWs (Supporting Information, Figure S5).

We have recently reported on the elaboration, by a similar solution chemistry approach, of a catalyst containing Co NWs grown on the surface of the Co nanoparticles of a reference Co/Al<sub>2</sub>O<sub>3</sub>-SiO<sub>2</sub> catalyst. That catalyst had shown an excellent stability under FTS conditions in a slurry reactor, despite the fact that the anisotropic shape was shown not to be conserved

**Table 1:** Comparison of the activity and selectivity for the cobalt/metallic foam catalyst with the reference catalyst (TOS = 75 h).

Catalyst	CO conversion [%]	Cobalt time yield [ $\times 10^{-3} \text{ mol}_{\text{Co}} \text{ mol}_{\text{Co}}^{-1} \text{ s}^{-1}$ ]	CH <sub>4</sub> [%]	C2–4 [%]	C5 + [%]	Olefins/Paraffins
Co/SiO <sub>2</sub> -Al <sub>2</sub> O <sub>3</sub>	24.5	5.8	26.0	16.2	57.8	0.114
hcp-Co/Cu <sub>foam</sub>	31.9	15.4	18.3	10.6	71.1	0.056

after catalysis.<sup>[17]</sup> The Co/Cu<sub>foam</sub> monolith is composed of Co NWs directly grown on substrates that can dissipate heat. They are therefore less prone to sintering. The catalytic performances of the hcp-Co/Cu<sub>foam</sub> monolith were evaluated for FTS in a fixed bed reactor (Table 1) and compared to the ones of a 15% Co/Al<sub>2</sub>O<sub>3</sub>-SiO<sub>2</sub> reference catalyst prepared by incipient wetness impregnation (see the Supporting Information for details).

The reference catalyst was diluted in SiO<sub>2</sub>-Al<sub>2</sub>O<sub>3</sub> to reach a loading (0.85% w/w) comparable to the hcp-Co/Cu<sub>foam</sub> catalyst and limit the creation of hot spots. The BET surface area of this catalyst is 128 m<sup>2</sup> g<sup>-1</sup> and a mean Co crystallite size of 14.7 nm was determined from XRD (from the corresponding d(Co<sub>3</sub>O<sub>4</sub>) (Supporting Information, Figure S6). In this catalyst, cobalt is crystallized mainly in the fcc phase, and the Co<sup>0</sup> amount after reduction is around 88% as estimated by temperature programmed reduction (TPR) analysis.<sup>[17]</sup> The diluted 15% Co/Al<sub>2</sub>O<sub>3</sub>-SiO<sub>2</sub> reference catalyst was reduced in situ under H<sub>2</sub> flow at 450°C during 16 h prior to FTS. No reduction step was needed for the Co/Cu<sub>foam</sub> catalyst, since the hcp-Co NWs are already purely metallic. In that case, the reactor was loaded in a glove box to avoid any oxidation. The FT tests were carried out at 220°C, with a total pressure of 10 bar, a H<sub>2</sub>/CO ratio of 2 and a CO flow of 10 mL min<sup>-1</sup> corresponding to a gas hourly space velocity (GHSV) of 890 h<sup>-1</sup>. Detailed results of the performance of the two catalysts at 75 h time on-stream (TOS) are presented in Table 1. The activity expressed as cobalt time yield (CTY) of the hcp-Co/Cu<sub>foam</sub> catalyst is significantly higher than that of the reference catalyst and of many reported Co-based catalysts (Supporting Information, Figure S7). Although it is easy to guess a very high value, the turnover frequency (TOF) of the hcp-Co/Cu<sub>foam</sub> catalyst cannot be accurately evaluated owing to: i) the impossibility to precisely measure the NWs dimensions from SEM and ii) the presence of ligands that prevent dispersion measurement by chemisorption. This significantly higher activity can be attributed to the choice of the support and/or to the structure of the catalyst (hcp-Co NWs).<sup>[4]</sup> Furthermore, as evidenced by the magnetic measurements, the cobalt in the Co/Cu<sub>foam</sub> catalyst is completely reduced, while in the reference catalyst part of the Co is oxidized. The evolution of CO conversion over the whole time period (75 h) is shown in the Supporting Information, Figure S8 and gives information on the stability over time of the hcp-Co/Cu<sub>foam</sub> catalyst compared to the reference catalyst. A tendency to a higher activity for the hcp-Co/Cu<sub>foam</sub> catalyst over time can be observed. The increase of Co/Cu<sub>foam</sub> catalyst activity over time could be the result of partial ligand removal during the reaction which liberates active sites previously occupied by the ligands. Indeed, we have previously shown that HDA/LA ligands can be removed upon treatment at 270°C under hydrogen.<sup>[17]</sup>

A lower selectivity towards methane and better selectivity to C5+ are obtained with the hcp-Co/Cu<sub>foam</sub> catalyst. This could be the result of the use of an “all metal” catalyst that avoids hot spots, which are known to negatively impact the selectivity, promoting CH<sub>4</sub> formation.<sup>[11,12,18]</sup> Indeed, heat and mass transfer phenomena that depend on the catalyst and on the reactor play a key role in FTS selectivity.<sup>[11a,19]</sup> It has been observed that the use of metallic foam as a support for FTS leads to improved heat and mass transfer in the reactor, accounting for low CH<sub>4</sub> production and high C5+ selectivity, respectively.<sup>[11a]</sup>

In another work, for large pore supports, the lower H/CO ratios chemisorbed on the catalyst active sites was found to be related to a limited CH<sub>4</sub> formation.<sup>[19a]</sup> The morphology of the spent Co/Cu<sub>foam</sub> catalyst after 75 hours TOS has been examined by SEM. It can be seen from Figure 3 that the Co NWs have conserved their shape and no sintering can be observed.

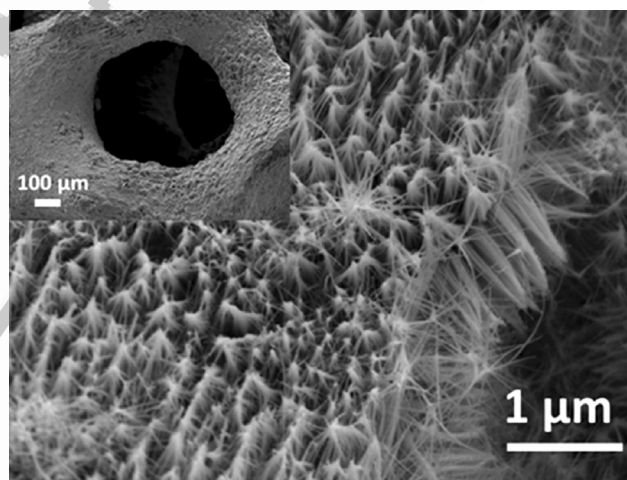


**Figure 3.** SEM image of the spent hcp-Co/Cu<sub>foam</sub> after 75 h TOS. Inset: a low magnification micrograph.

The XRD diffractogram of the spent Co/Cu<sub>foam</sub> catalyst shows that the cobalt hcp structure has been conserved (Supporting Information, Figure S9). The conservation of the morphology as well as the crystal structure can explain the catalytic performance and stability over 75 hours TOS.

To generalize our synthetic strategy, the growth of cobalt was also performed on another metal, namely nickel. The main characteristics and a SEM image of the nickel foam before Co growth are given in the Supporting Information, Figure S10. In Figure 4, we present the SEM images of the Ni foam after Co NW growth. The diffraction pattern of the Co/Ni<sub>foam</sub> also shows the characteristic peaks of the hcp-Co (Supporting Information, Figure S11). ICP-AES analyses

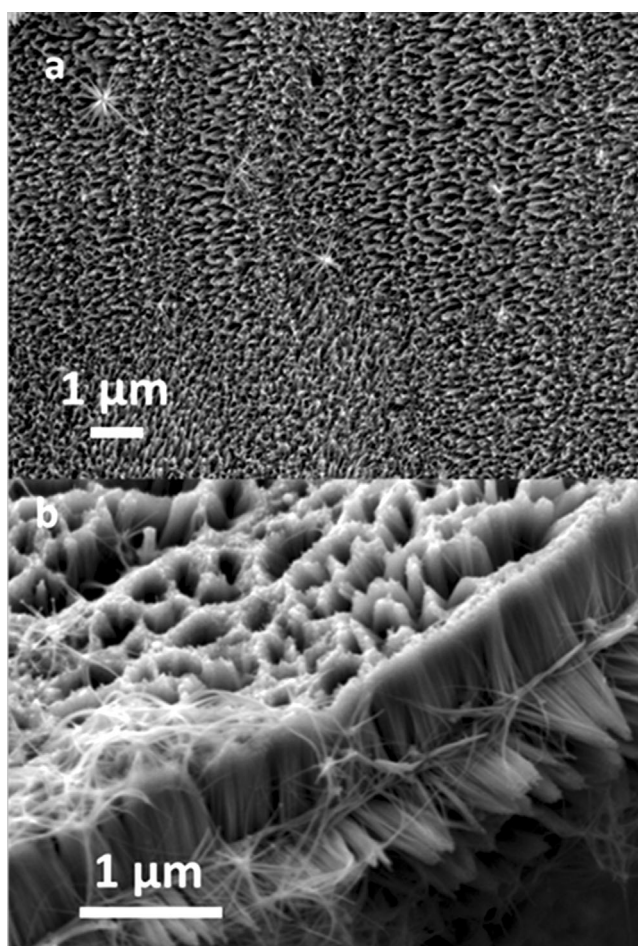


**Figure 4.** SEM images of the Co/Ni<sub>foam</sub> monolith: a) low and b) higher magnification.

performed on this sample showed a 1.45% w/w cobalt loading. The XPS analyses (Supporting Information, Figure S12) show the presence of Ni oxides on the bare Ni foam. After Co growth, the signals of Ni have almost completely disappeared because of the Co masking the Ni foam surface. As for the Co/Cu<sub>foam</sub> catalyst, the cobalt is mainly present on the Co/Ni<sub>foam</sub> sample as Co<sup>0</sup>.

In summary, we have employed a solution-based approach for the direct growth of dense arrays of *hcp*-cobalt NWs with length up to 1 μm on copper and nickel foams. The Co/Cu<sub>foam</sub> catalyst was investigated for the FTS and presented a much higher activity and a higher C5+ selectivity than a Co/Al<sub>2</sub>O<sub>3</sub>-SiO<sub>2</sub> reference catalyst. This nanostructured material shows remarkable performances and a stable active phase under FT conditions in fixed bed reactor that should be attributed to the use of metallic foam as support, which allows a better management of exothermicity, thus limiting CH<sub>4</sub> formation and favoring chain propagation. Another possibility is that the NWs structure plays a role in the Co-Cu<sub>foam</sub> catalyst performances. The *hcp*-Co phase is assumed to be more active than the *fcc*-one, this being probably an additional reason for the increased performances.

Growing Co NWs on foams of varying heat capacities could help concluding on this aspect. The robust *hcp*-Co-Cu

interface as well as the rapid dissipation of the heat of reaction from the catalyst particles, did avoid its overheating and sintering. These new catalytic systems offer promising perspectives for FTS, but could be also of interest for other reactions, in fixed-bed or microreactors. Further experiments are in course to significantly increase the Co loading on different metallic foams and broaden the spectrum of catalytic reactions.

### Acknowledgements

J.H. thanks the Université de Toulouse (Nysfit project No. 6013) and the Région Midi Pyrénées (Nysfit project No. 13050269) for financial support. M.E. thanks the EC (HyCoRod project, H2020-MSCA-IF 2015 No. 704098). S. Pinaud is acknowledged for assistance with the set-up.

### Conflict of interest

The authors declare no conflict of interest.

**Keywords:** cobalt · Fischer–Tropsch synthesis · *hcp* structures · metallic foams · nanowires

- [1] O. O. James, B. Chowdhury, M. A. Mesubi, S. Maity, *RSC Adv.* **2012**, *2*, 7347–7366.
- [2] M. E. Dry, *Catal. Today* **2002**, *71*, 227–241.
- [3] A. Y. Khodakov, W. Chu, P. Fongarland, *Chem. Rev.* **2007**, *107*, 1692–1744.
- [4] F. Diehl, A. Y. Khodakov, *Oil Gas Sci. Technol.* **2009**, *64*, 11–24.
- [5] a) G. L. Bezemer, J. H. Bitter, H. P. C. E. Kuipers, H. Oosterbeek, J. E. Holewijn, X. Xu, F. Kapteijn, A. J. van Dillen, K. P. de Jong, *J. Am. Chem. Soc.* **2006**, *128*, 3956–3964; b) J. P. den Breejen, P. B. Radstake, G. L. Bezemer, J. H. Bitter, V. Frøseth, A. Holmen, K. P. de Jong, *J. Am. Chem. Soc.* **2009**, *131*, 7197–7203; c) W. T. Ralston, G. Melaet, T. Saephan, G. A. Somorjai, *Angew. Chem. Int. Ed.* **2017**, *56*, 7415–7419; *Angew. Chem.* **2017**, *129*, 7523–7527; d) P. van Helden, I. M. Ciobîcă, R. L. J. Coetzer, *Catal. Today* **2016**, *261*, 48–59.
- [6] J.-X. Liu, P. Wang, W. Xu, E. J. M. Hensen, *J. Eng.* **2017**, *3*, 467–476.
- [7] J.-X. Liu, H.-Y. Su, D.-P. Sun, B.-Y. Zhang, W.-X. Li, *J. Am. Chem. Soc.* **2013**, *135*, 16284–16287.
- [8] a) G. Kwak, D.-E. Kim, Y. T. Kim, H.-G. Park, S. C. Kang, K.-S. Ha, K.-W. Jun, Y.-J. Lee, *Catal. Sci. Technol.* **2016**, *6*, 4594–4600; b) H.-Y. Su, Y. Zhao, J.-X. Liu, K. Sun, W.-X. Li, *Catal. Sci. Technol.* **2017**, *7*, 2967–2977; c) H. Karaca, O. V. Safonova, S. Chambrey, P. Fongarland, P. Roussel, A. Griboval-Constant, M. Lacroix, A. Y. Khodakov, *J. Catal.* **2011**, *277*, 14–26; d) D. Enache, B. Rebours, M. R. Auberger, R. Revel, *J. Catal.* **2002**, *205*, 346–353.
- [9] V. V. Matveev, D. A. Baranov, G. Y. Yurkov, N. G. Akatiev, I. P. Dotsenko, S. P. Gubin, *Chem. Phys. Lett.* **2006**, *422*, 402–405.
- [10] N. E. Tsakoumis, M. Rønning, Ø. Borg, E. Rytter, A. Holmen, *Catal. Today* **2010**, *154*, 162–182.
- [11] a) J. C. Park, N. S. Roh, D. H. Chun, H. Jung, J. Yang II, *Fuel Process. Technol.* **2014**, *119*, 60–66; b) C. G. Visconti, E. Tronconi, L. Lietti, G. Groppi, P. Forzatti, C. Cristiani, R.

- 1 Zennaro, S. Rossini, *Appl. Catal. A* **2009**, *370*, 93–101; c) L.  
2 Giani, G. Groppi, E. Tronconi, *Ind. Eng. Chem. Res.* **2005**, *44*,  
3 9078–9085; d) S. T. Kolaczowski, S. Awdry, T. Smith, D.  
4 Thomas, L. Torkuhl, R. Kolvenbach, *Catal. Today* **2016**, *273*,  
5 221–233; e) S. Razza, T. Heidig, E. Bianchi, G. Groppi, W.  
6 Schwieger, E. Tronconi, H. Freund, *Catal. Today* **2016**, *273*, 187–  
7 195.
- [12] a) B. Todić, V. V. Ordonsky, N. M. Nikacevic, A. Y. Khodakov,  
8 D. B. Bukur, *Catal. Sci. Technol.* **2015**, *5*, 1400–1411; b) H. J.  
9 Robota, L. A. Richard, S. Deshmukh, S. LeViness, D. Leonarduzzi,  
10 D. Roberts, *Catal. Surv. Asia* **2014**, *18*, 177–182.
- [13] B. Cormary, F. Dumestre, N. Liakakos, K. Soulantica, B.  
11 Chaudret, *Dalton Trans.* **2013**, *42*, 12546–12553.
- [14] a) F. Dumestre, B. Chaudret, C. Amiens, M.-C. Fromen, M.-J.  
12 Casanove, P. Renaud, P. Zurcher, *Angew. Chem. Int. Ed.* **2002**,  
13 *41*, 4286–4289; *Angew. Chem.* **2002**, *114*, 4462–4465; b) N.  
14 Liakakos, B. Cormary, X. Li, P. Lecante, M. Respaud, L. Maron,  
15 A. Falqui, A. Genovese, L. Vendier, S. Koïnis, B. Chaudret, K.  
16 Soulantica, *J. Am. Chem. Soc.* **2012**, *134*, 17922–17931; c) B.  
17 Cormary, T. Li, N. Liakakos, L. Peres, P.-F. Fazzini, T. Blon, M.  
18 Respaud, A. J. Kropf, B. Chaudret, J. T. Miller, E. A. Mader, K.  
19 Soulantica, *J. Am. Chem. Soc.* **2016**, *138*, 8422–8431.
- [15] a) N. Liakakos, T. Blon, C. Achkar, V. Vilar, B. Cormary, R. P.  
20 Tan, O. Benamara, G. Chaboussant, F. Ott, B. Warot-Fonrose, E.  
21 Snoeck, B. Chaudret, K. Soulantica, M. Respaud, *Nano Lett.*  
22 **2014**, *14*, 3481–3486; b) N. Liakakos, C. Achkar, B. Cormary, J.  
23 Harmel, B. Warot-Fonrose, E. Snoeck, B. Chaudret, M.  
24 Respaud, K. Soulantica, T. Blon, *ACS Nano* **2015**, *9*, 9665–9677.
- [16] J. Nogués, I. K. Schuller, *J. Magn. Magn. Mater.* **1999**, *192*, 203–  
25 232.
- [17] J. Harmel, A. Berliet, K. Dembélé, C. Marcelot, A.-S. Gay, O.  
26 Ersen, S. Maury, A. Fécant, B. Chaudret, P. Serp, K. Soulantica,  
27 *ChemCatChem* **2018**, *10*, 1614–1619.
- [18] Y. Liu, I. Florea, O. Ersen, C. Pham-Huu, C. Meny, *Chem.*  
28 *Commun.* **2015**, *51*, 145–148.
- [19] a) J. A. Lapszewicz, H. J. Loeh, J. R. Chipperfield, *J. Chem. Soc.*  
29 *Chem. Commun.* **1993**, 913–914; b) E. Iglesia, *Appl. Catal. A*  
30 **1997**, *161*, 59–78.

Manuscript received: April 27, 2018

Revised manuscript received: June 7, 2018

Accepted manuscript online: June 12, 2018

Version of record online: ■■■■■, ■■■■■

## Communications

## Metallic Foams

J. Harmel, L. Peres, M. Estrader,  
A. Berliet, S. Maury, A. Fécant,  
B. Chaudret, P. Serp,\*  
K. Soulantica\*     

*hcp*-Co Nanowires Grown on Metallic  
Foams as Catalysts for Fischer–Tropsch  
Synthesis



**Foaming at the catalyst:** Cobalt nano-  
wires have been grown on metallic foams.  
The *hcp*-Co/Cu<sub>foam</sub> catalyst is remarkably  
stable, active, and selective in Fischer–  
Tropsch synthesis.

## Metallschäume

J. Harmel, L. Peres, M. Estrader,  
A. Berliet, S. Maury, A. Fécant,  
B. Chaudret, P. Serp,\*  
K. Soulantica\*     

*hcp*-Co Nanowires Grown on Metallic  
Foams as Catalysts for Fischer–Tropsch  
Synthesis



**Schäumende Katalyse:** Cobalt-Nano-  
drähte wurden auf Metallschäumen  
erzeugt. Der *hcp*-Co/Cu-Schaum-  
(„foam“)-Katalysator ist bemerkenswert  
stabil, aktiv und selektiv in der Fischer-  
Tropsch-Synthese.

Please check that the ORCID identifiers listed below are correct. We encourage all authors to provide an ORCID identifier for each coauthor. ORCID is a registry that provides researchers with a unique digital identifier. Some funding agencies recommend or even require the inclusion of ORCID IDs in all published articles, and authors should consult their funding agency guidelines for details. Registration is easy and free; for further information, see <http://orcid.org/>.

Dr. Justine Harmel <http://orcid.org/0000-0003-2341-3281>

Laurent Peres

Dr. Marta Estrader

Adrien Berliet <http://orcid.org/0000-0002-8914-3213>

Dr. Sylvie Maury <http://orcid.org/0000-0002-7742-8385>

Dr. Antoine Fécant <http://orcid.org/0000-0003-2059-8778>

Dr. Bruno Chaudret <http://orcid.org/0000-0001-9290-6421>

Prof. Dr. Philippe Serp <http://orcid.org/0000-0003-1424-2724>

Dr. Katerina Soulantica <http://orcid.org/0000-0003-3033-1620>